Report

Cell Reports

Helicobacter pylori Infection Causes Characteristic DNA Damage Patterns in Human Cells

Graphical Abstract

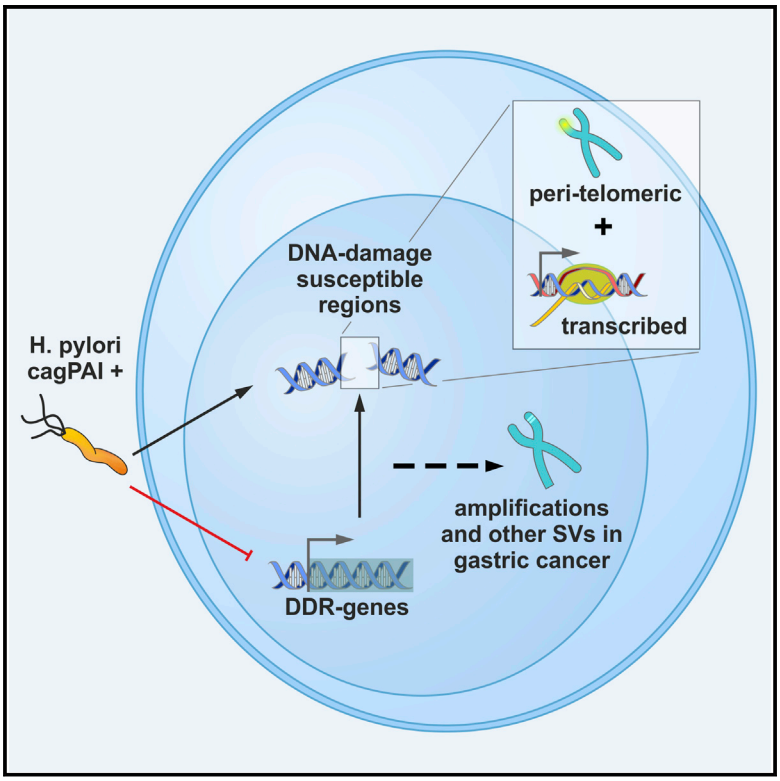

Authors

Max Koeppel, Fernando Garcia-Alcalde, Frithjof Glowinski, Philipp Schlaermann, Thomas F. Meyer

Correspondence

meyer@mpiib-berlin.mpg.de

In Brief

The gastric pathogen *H. pylori* can cause cancer in humans by compromising the genomic integrity of infected cells. Koeppel et al. show that infection affects the DNA damage response and reveal a DNA damage pattern reminiscent of genomic aberrations found in gastric tumors.

Highlights

- *H. pylori* impairs the DNA repair response in normal human epithelial cells
- Distinct genomic regions show increased susceptibility to *H. pylori*-induced damage
- DNA damage accumulates in telomere-proximal, actively transcribed regions
- Susceptible genomic regions overlap with gastric cancer genomic aberrations

Accession Numbers

GSE55699

Koeppel et al., 2015, Cell Reports *11*, 1703–1713
June 23, 2015
http://dx.doi.org/10.1016/j.celrep.2015.05.030

Cell Reports
Report

Helicobacter pylori Infection Causes Characteristic DNA Damage Patterns in Human Cells

Max Koeppel,[1] Fernando Garcia-Alcalde,[1] Frithjof Glowinski,[1] Philipp Schlaermann,[1] and Thomas F. Meyer[1,*]
[1]Department of Molecular Biology, Max Planck Institute for Infection Biology, Charitéplatz 1, 10117 Berlin, Germany
*Correspondence: meyer@mpiib-berlin.mpg.de
http://dx.doi.org/10.1016/j.celrep.2015.05.030

SUMMARY

Infection with the human pathogen *Helicobacter pylori* (*H. pylori*) is a major risk factor for gastric cancer. Since the bacterium exerts multiple genotoxic effects, we examined the circumstances of DNA damage accumulation and identified regions within the host genome with high susceptibility to *H. pylori*-induced damage. Infection impaired several DNA repair factors, the extent of which depends on a functional cagPAI. This leads to accumulation of a unique DNA damage pattern, preferentially in transcribed regions and proximal to telomeres, in both gastric cell lines and primary gastric epithelial cells. The observed pattern correlates with focal amplifications in adenocarcinomas of the stomach and partly overlaps with known cancer genes. We thus demonstrate an impact of a bacterial infection directed toward specific host genomic regions and describe underlying characteristics that make such regions more likely to acquire heritable changes during infection, which could contribute to cellular transformation.

INTRODUCTION

Eukaryotic genomes are under constant challenge from environmental influences that threaten their integrity. Among the agents that can alter both genetic and epigenetic features of a cell, the gastric bacterium *H. pylori* has a prominent role during the development of stomach adenocarcinoma (Peek and Crabtree, 2006).

Contributing to the infection-associated pathogenicity is the *cag* pathogenicity island (cagPAI), a multigene locus encoding a type IV secretion system (T4SS) and corresponding factors that are translocated into host cells (Backert et al., 2000; Odenbreit et al., 2000), among them the cytotoxin-associated gene A (CagA). CagA has been reported to cause chromosomal instability (CIN) (Umeda et al., 2009), which might contribute to the increased cancer risk posed by CagA-positive *H. pylori* (Blaser et al., 1995; Parsonnet et al., 1997). Apart from chronic inflammation (Fox and Wang, 2007), *H. pylori* also seems to cause increased point mutation rates in mouse models during infection (Jenks et al., 2003; Touati et al., 2003). This process has been linked to reduced expression of mismatch repair genes (Kim et al., 2002) and increased expression of activation-induced cytidine deaminase (AID) (Matsumoto et al., 2007). *H. pylori* can also induce DNA double-strand breaks (DSBs), which in turn leads to activation of checkpoint activities, including the recruitment of 53BP1 or ATM to DNA damage foci (Chaturvedi et al., 2011; Toller et al., 2011).

Genomic characterization of gastric cancers has identified recurrent mutations in coding regions of genes and has partly illuminated their contribution to tumor progression (Wang et al., 2011; Zang et al., 2012). Whole genome studies have cataloged somatic copy number alterations (SCNAs) (Dulak et al., 2012; Hillmer et al., 2011) and enabled detailed molecular characterization of gastric tumors (TCGA Research Network, 2014a; Wang et al., 2014). Although some of these studies tried to evaluate the role of *H. pylori* in these processes, it has remained difficult to provide a strict causal relationship between genome-wide mutation profiles and infection due to the multistep process of gastric carcinogenesis (Correa and Piazuelo, 2012) and the long time—usually decades—between the initial infection and tumor formation (Bauer and Meyer, 2011), which allows extensive positive selection of cells with mutation-derived growth advantages and additional evolutionary processes to occur.

To illuminate the early events affecting genomic integrity upon infection and the mechanisms of *H. pylori*-mediated genomic damage, we analyzed the host genomic regions primarily damaged upon infection and the DNA damage response (DDR). Overall, we found reduced levels and activity of several DDR factors, resulting in a unique DDR pattern distinct from that observed with other genotoxic agents. Failure to initiate repair pathways was partially dependent on the presence of CagPAI. DNA damage was found to accumulate at the end of chromosomal arms and correlate with genic and transcribed regions. Furthermore, with prolonged infection time, the pattern of DNA damage resembles that of structural variations (SVs) in gastric cancers and correlates with recurrent focal amplifications in gastric adenocarcinomas.

RESULTS

Extent of Host Response to Genomic Damage during *H. pylori* Infection

To gain insight into the events underlying the genomic damage, we compared the DDR after infection with that of other genotoxic

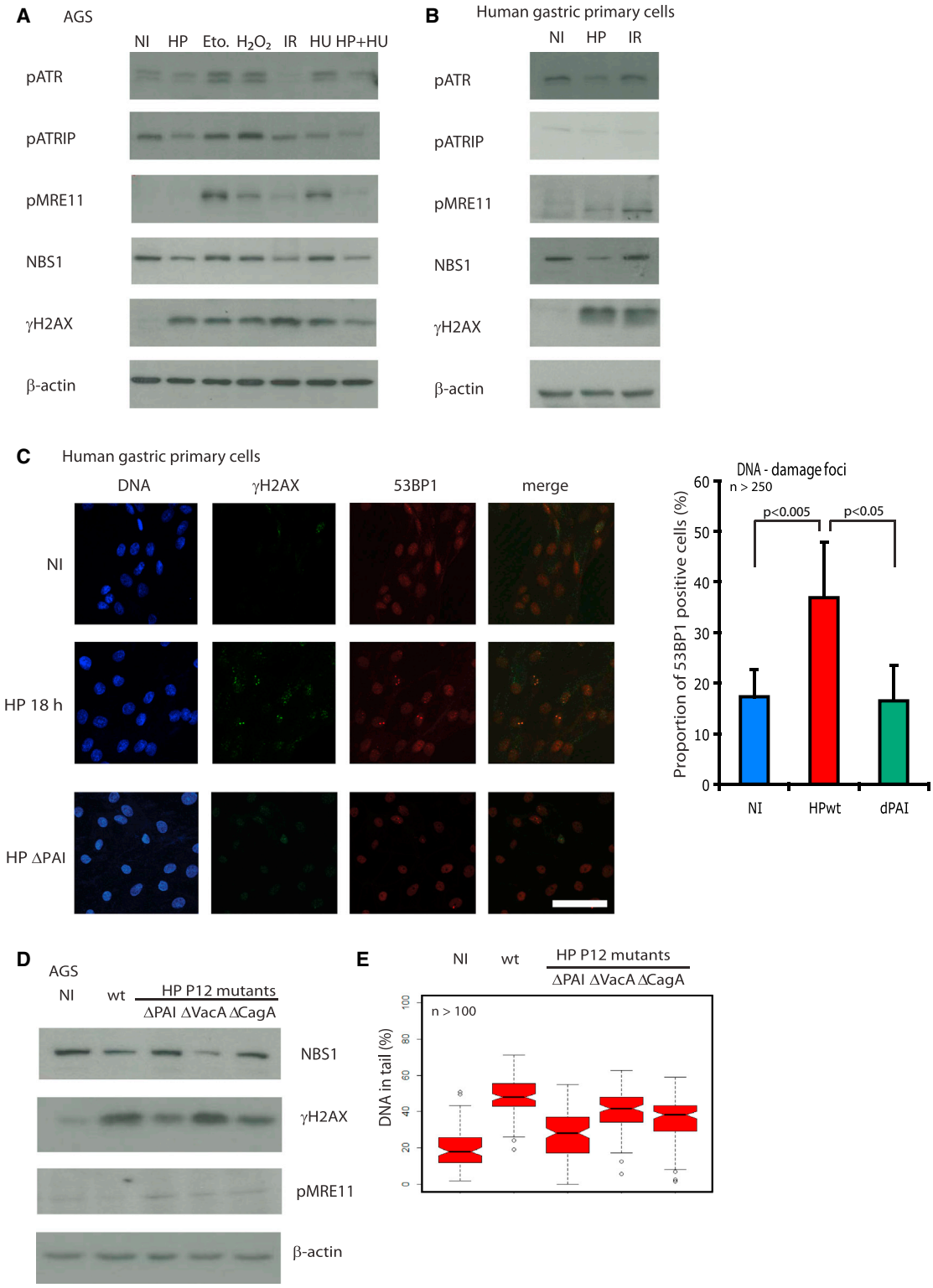

Figure 1. Differential Responses of Host Cells to DNA Damage Caused by *H. pylori* or Genotoxic Treatments

(A) AGS cells were infected with P12 (MOI 50) for 18 hr and/or subjected to the indicated treatment or left untreated (NI). Western blotting shows comparable induction of γH2AX, while activity and abundance of several DDR-proteins are specifically decreased.

(B) Primary human epithelial cells were infected with P12 for 18 hr (MOI 25) or subjected to IR prior to western blot analysis, showing a similar impairment of DDR activation after infection as in (A).

(legend continued on next page)

treatments. Cells were either infected with *H. pylori* strain P12 at multiplicity of infection (MOI) 50 or treated with 10 μM etoposide (Eto), 250 mM H_2O_2, 10 Gy gamma irradiation (IR), or 10 mM hydroxy-urea (HU) for 18–20 hr to induce different types of DNA damage and corresponding repair pathways. Although all treatments caused comparable induction of the DNA damage marker γH2AX, other DDR proteins were differentially activated (Figure 1A). While the mutagens caused phosphorylation of ATR and MRE11, this activation was blocked after infection. Infection also impaired phosphorylation of the ATR interacting protein ATRIP and reduced levels of NBS1/NBN protein, which together with MRE11 forms part of the MRN complex. Interestingly, if infected cells were also treated with HU, the DDR was impaired compared with HU treatment alone.

To enable further analysis, we carefully defined conditions under which the overall damage during infection was similar to that induced by IR. Following infection of gastric AGS and MKN74 cells, we observed an accumulation of γH2AX as early as 6-hr post-infection (p.i.), which by 18-hr p.i. reached levels comparable to those induced by 10 Gy IR (Figure S1A). The amount of broken DNA similarly accumulated over time, although we observed some differences between AGS and MKN74 cells (Figure S1B). Breaks accumulated in AGS cells during the first hours, reaching a steady state between 6- and 18-hr p.i., most likely due to a balance between repair and damage. In MKN74 cells, this process appeared delayed, although the amount of broken DNA at 18-hr p.i. was comparable to IR-induced damage.

Since the use of cancer cell lines may limit the conclusions we can draw about the role of *H. pylori* during transformation, we also infected 2D monolayer cultures of non-transformed human primary gastric epithelial cells, derived from 3D gastric spheroids established from isolated healthy gastric glands (Schlaermann et al., 2014). In these cells, γH2AX accumulated to a similar extent as observed after IR in AGS cells (Figure 1B), while the decrease in NBS1 and phosphorylated ATR was also comparable to that observed in AGS cells. However, the DNA damage mediator 53BP1 was recruited to damaged sites in primary epithelial cells (Figure 1C), indicating that not all responses to DNA damage after infection are hampered. Interestingly, an isogenic *Helicobacter* strain lacking the pathogenicity island failed to cause similar levels of DNA damage and 53BP1 recruitment in non-transformed cells (Figure 1C).

To examine which pathogen determinants contribute to the DNA damage and suppression of DDR pathways, we infected AGS cells with P12 or several isogenic derivatives lacking the T4SS and associated proteins (Figure 1D). CagA-positive strains caused a more prominent reduction in NBS1 levels and also had some specific effects on the phosphorylation of MRE11. In contrast to primary cells, infections with all strains led to some induction of γH2AX and accumulation of broken DNA, as shown by single-cell gel electrophoresis (Comet assay, Figure 1E), although the increase in damage was more prominent with CagA-positive strains. To evaluate this further, we examined putative host factors. As a major interacting partner, the phosphatase SHP2 is known to mediate several effects of CagA (Hatakeyama, 2014). Reducing its abundance with different siRNAs caused a modest, but reproducible increase in the amount of γH2AX (Figure S1C). We thus assume that the pathogenicity island causes multiple effects that accumulate to the increased damage observed, although there also seem to be cagPAI-independent effects.

Since 53BP1 localizes to discrete foci during G1-phase of the cell cycle (Pombo et al., 1998) and *H. pylori* has been reported to cause G1/S-arrest (Ding et al., 2008; Kim et al., 2010), we looked for possible effects in this regard. As the G1-arrest-inducing p21/CDKN1A was upregulated by 6-hr p.i. (Figure S1D), we tested whether the 53BP1 foci correspond to Oct1/PTF/transcription (OPT) bodies (Pombo et al., 1998). Indeed, some foci contained the OPT-body component Oct1 and were localized at the periphery of promyelocytic leukemia protein (PML) bodies (Pombo et al., 1998) (Figure S1E). Nevertheless, we did not detect changes in the number and size of OPT and PML bodies between uninfected and infected cells, indicating that different 53BP1 foci form upon infection.

H. pylori Suppresses DDR Factors on the Transcriptional Level

To elucidate the events responsible for the reduction in DDR activity, we extended our study to prolonged infections. From 18-hr p.i., we detected a time-dependent decrease of NBS1 (Figure 2A). To examine whether this occurred on a transcriptional level or was due to protein degradation, we treated cells with the proteasome inhibitor MG132 for 4 hr at the end of the infection period. NBS1 protein levels in infected cells were not restored to those of uninfected cells, however (Figure 2B), suggesting the involvement of additional transcriptional mechanisms. To explore this further, we obtained transcriptional information from two replicates of primary human gastric cells using RNA-seq. Comparing the expression of 179 genes implicated in various DDR pathways (Lange et al., 2011) in uninfected and infected cells, we identified 58 genes downregulated more than 2-fold, among them *NBS1*, *ATR*, *MLH1*, and *TP53* (Figure 2C). Only 11 genes of this list of DDR factors were upregulated to a similar extent; thus, we conclude that *H. pylori* causes a systematic reduction in DNA repair capacities.

(C) Representative confocal immunofluorescence of primary human gastric epithelial cells infected as in (B) with WT P12 or the isogenic ΔPAI strain shows DNA damage foci containing both γH2AX (green) and 53BP1 (red) only upon infection with the WT. Nuclei visualized with Draq5. Scale bar represents 50 μm. IF for the lower was carried out separately. (Right) Absolute quantification of DNA damage foci in cells as shown on the left (error bars indicate SD from three independent experiments, and p values are derived from Student's t test).

(D) AGS cells were infected for 18 hr (MOI 50) with WT P12 or its isogenic ΔPAI, Δ*VacA*, and Δ*CagA* deletion mutants, followed by protein analysis showing dependency of γH2AX accumulation and NBS1 inhibition on functional cagPAI.

(E) Box and whisker plot showing the extent of DNA damage induced by different isogenic *H. pylori* mutants as determined by Comet assay; infections were performed as in (D).

See also Figure S1.

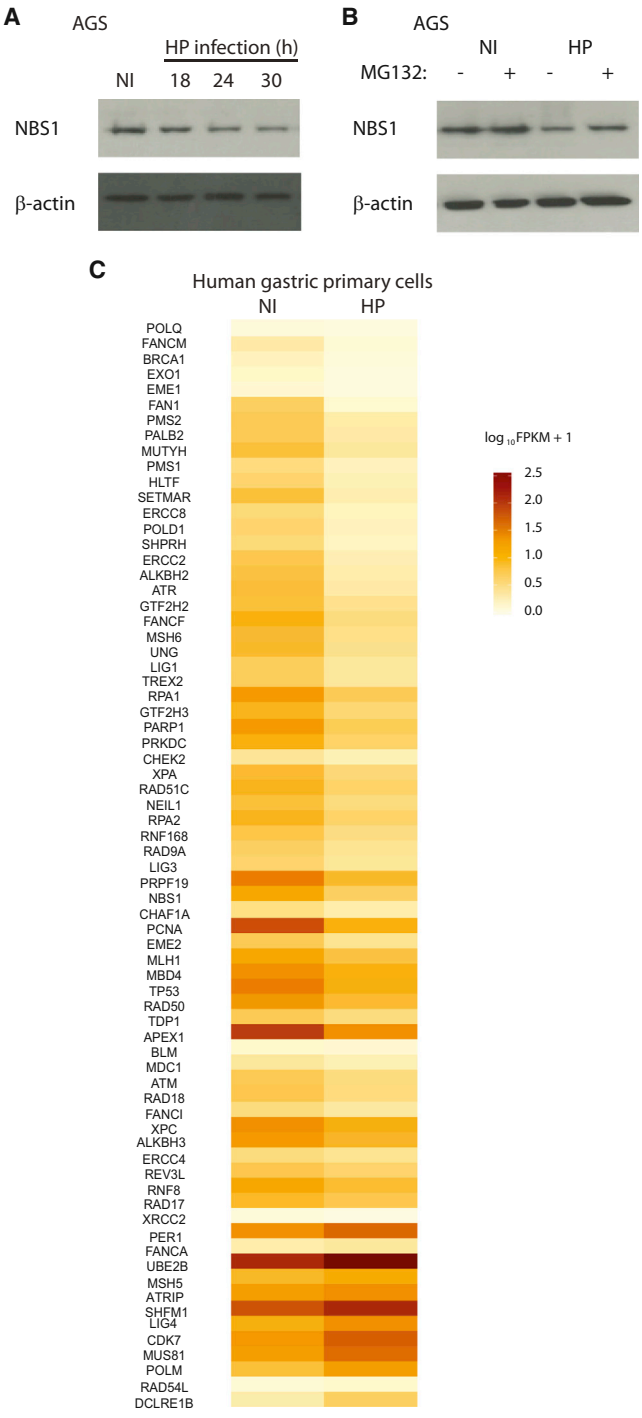

Figure 2. *H. pylori* Causes a Time-Dependent Transcriptional Decrease in DNA Damage Repair Factors

(A) AGS cells were infected with *H. pylori* strain P12, and levels of NBS1 were analyzed by western blot, showing a time-dependent decrease in protein levels. (B) Infected AGS cells were treated with MG132 for 4 hr to inhibit protein degradation, which does not restore the levels of NBS1 to that of uninfected cells. (C) Primary human gastric epithelial cells were infected with *H. pylori* followed by RNA-seq analysis of proteins involved in DDR. Shown are proteins changing their expression at least 2-fold, of which the majority shows reduced expression.

H. pylori-Specific Damage Spreads from Telomeres and Correlates with Active Transcription

Next, we asked whether such a global impairment of DDR factors could lead to site-specific accumulation of broken DNA in host cells since this would have consequences for genome integrity. We compared *H. pylori*- with IR-induced damage because it triggered a similar DDR but induces DSBs in a random fashion. Having defined conditions under which the bacteria-induced DNA damage reached a similar extent as that induced by IR, our aim was to identify host genomic regions that were at high risk of being damaged during infection. Thus, we performed chromatin immunoprecipitation (ChIP)-seq experiments in AGS cells targeting γH2AX and the associated DNA. We compared an early (6-hr p.i.) and a late (18-hr p.i.) time point with γH2AX-derived DNA from irradiated and control cells to obtain genome-wide localization information from two biological replicates. Using HOMER (Heinz et al., 2010) to identify globally enriched regions, we found damaged genomic loci across all chromosomes and conditions, also in uninfected AGS cells (Figures S2A and S2B).

To test for reproducibility between the biological replicates, we applied the ENCODE guidelines (Landt et al., 2012) and found an overall good performance (Table S1). This similarity was also confirmed when we annotated enriched regions of each replicate to the Refseq database and found only small variation between them (Figure 3A). Intriguingly, we found different distributions of signal accumulation in control and infected cells, with a large shift toward genic regions at prolonged infection times, in contrast to the location of damage generated by IR.

Since the control cells also displayed damaged regions, we wondered whether infection enhances damage at existing lesions or changes the signal distribution toward new sites. Comparing overlapping and unique sites of uninfected versus 18-hr infected cells showed that most of the damaged sites between the two conditions seemed to locate within unique regions; thus, we assumed that there is mainly a shift in the signal upon infection (Figure S2C). Moreover, the extent of damage increased at sites unique to infection, while common sites present in both conditions seemed to accumulate slightly less damage (Figure 3B). The OPT bodies we identified suggested that the signal in uninfected cells might result from damage at fragile sites, which may overlap with the damaged sites identified (Harrigan et al., 2011). Fragile sites have been classified as either common fragile sites (CFSs) (Glover, 2006), or early replicating fragile sites (ERFSs) (Barlow et al., 2013), both with slightly different characteristics. For comparison, we used genome-wide sets of CFS and ERFS (Barlow et al., 2013; Crosetto et al., 2013). Around 10% of damaged regions in all conditions showed an overlap with fragile sites, which is higher than expected for CFS, and we observed an even greater enrichment at ERFS (Figure S2D), although there was no specific effect of infection, in line with our observation that OPT bodies did not change between conditions.

Because *H. pylori*-susceptible areas were enriched in genic regions, we specifically examined genes expressed in the same cell line using an in-house derived RNA-seq dataset (F.G. and T.F.M., unpublished data). We found a significant correlation between actively transcribed genes and regions of

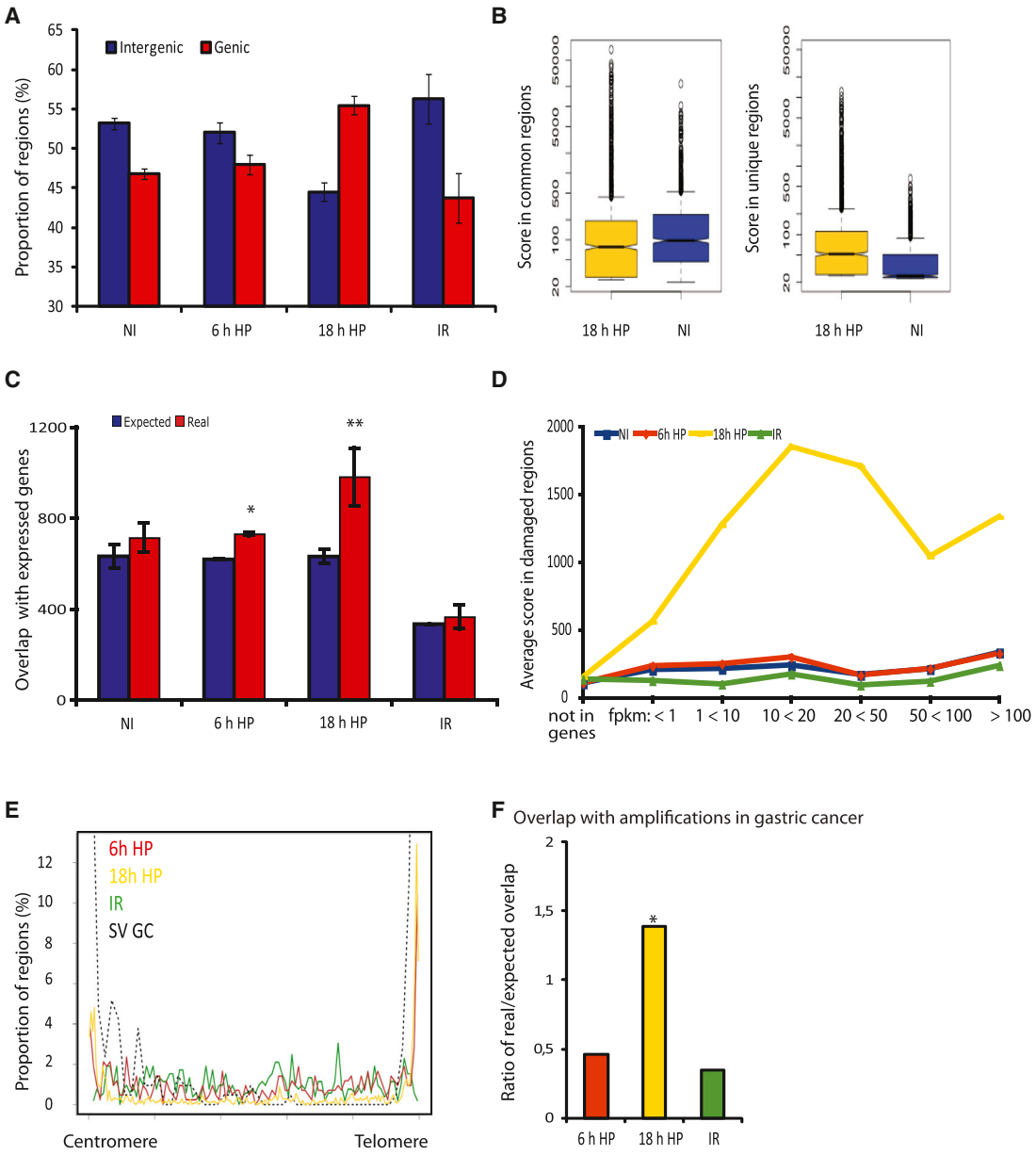

Figure 3. Global Analysis of γH2AX-ChIP-seq Shows that Regions with Active Gene Transcription Close to Telomeres Are Susceptible to *H. pylori*-Induced Damage and Overlap with SVs in Gastric Cancers

(A) Annotation of damaged regions to the RefSeq-database indicates that infection-induced damage preferentially accumulates in genic regions (error bars indicate SD and were derived from the individual annotation of the two global biological replicates).

(B) Damaged regions of non-infected cells and 18-hr p.i. depicting the damage score of unique and overlapping regions, indicating an increase in damage 18-hr p.i., particularly in unique regions.

(C) The individual sets of damaged regions were intersected with expression data from RNA-seq of AGS cells and displayed as the ratio between real versus expected random overlap. Expressed genes were defined by >5 FPKM (Cufflinks analysis) (*$p < 10^{-5}$, **$p < 10^{-15}$); hypergeometric distribution testing; error bars are as in (A).

(D) The average HOMER score corresponding to the extent of damage, across regions with various levels of transcription, showing an increase at 18-hr p.i.

(E) Enriched DNA damage for the infected and the irradiated samples compared with untreated cells was calculated and the signal plotted over the chromosomal arms, separated into equal numbers of bins. Enriched signals for *H. pylori*-susceptible regions were found at the end of chromosomal arms, whereas IR-induced signal was distributed randomly. Global distribution of SVs from gastric cancer shows a pattern similar to that caused by infection.

(F) Hypergeometric distribution testing was performed on the individual enriched regions compared with recurrent focal amplifications from gastric cancer studies, indicating a significant overlap (*$p < 0.0005$).

See also Figure S2 and Table S1.

Table 1. Genomic Location of Genes with Known Cancer-Associated Functions that Overlap with Regions Damaged by *H. pylori*

Gene Name	Genomic Location
IRF4/DUSP2	chr6: 142755–518724
ZNF132	chr19: 58777980–59118881
AXIN1	chr16: 274256–474604
TFDP1	chr13: 114211207–114326395
MTCP1	ChrX: 154270854–154334882
FANCA	chr16: 89809224–89844072
TRIM7	chr5: 180618959–180660380
KDM5A	chr12: 430699–438398
BCL3	chr19: 45251978–45,263,301
POLE	chr12: 133237426–133241288
TFPT	chr19: 54610507–54613007
AKT2	chr19: 40757499–40763374
ERCC2	chr19: 45845159–45883309
CIC	chr19: 42789404–42793807
ZMYND8	chr20: 45978187–45982066
EPPK1	chr8: 144938736–144942401
DIDO1	chr20: 61565155–61568288
COL18A1	chr21: 46931285–46933785
PLCG1	chr20: 39772200–39774700
FOXA1	chr14: 38059419–38061919

H. pylori-induced DNA damage at 18-hr p.i. (average of 983 real versus 632 expected; $p < 10^{-15}$), which was not seen in any other condition (Figure 3C). Additionally, we used the HOMER scores of the different regions to compare the extent of specific damage in differentially transcribed regions in AGS cells. Separating expressed genes into several bins according to their expression level, we found that the 18-hr infection already caused a clear increase in the average damage score in genic but non-expressed regions, which was even more pronounced in transcribed genes (Figures 3D and S2E).

Because of this shift in signal localization and to focus on regions enriched in DNA damage upon infection or IR, we performed a differential analysis of each condition compared with the control to remove signals already present in uninfected conditions. To further characterize regions damaged by *H. pylori*, we plotted their distribution across the chromosomal arms and compared the enriched regions with a dataset of SV in gastric cancer (Wang et al., 2014). Only infection-induced damage accumulated preferentially in telomere-proximal regions (around 10% of all regions) and partly also in regions close to the centromeres (around 5% of all regions) (Figure 3E). This appears very similar to the pattern of SVs obtained from gastric cancer sequencing. Because such a pattern may also occur in cancers not induced by bacteria, we examined whole genome sequence data from three additional studies that analyzed at least 20 donors for SVs (Baca et al., 2013; Berger et al., 2012; TCGA Research Network, 2014b). The accumulated SVs from melanoma and lung adenocarcinoma distribute randomly across chromosomal arms, while only SVs from prostate cancer show a similar pattern to the *H. pylori*-induced DNA damage (Figure S2F). To focus on recurrent events, we included another genomic gastric cancer study (TCGA Research Network, 2014a) and compared patterns of focal amplifications/deletions with the *H. pylori*-induced damage. Surprisingly, there was a unique correlation between prolonged infection and recurrent amplifications (111 real versus 80 expected; $p < 0.0005$) that was not seen with the IR-induced damage (Figure 3F). Since these regions might have an impact on cellular transformation, we tested a putative correlation with genes in these regions previously implicated in cancer. To this end, we compiled a non-redundant list of known cancer-associated genes from the Cancer Gene Census (Futreal et al., 2004), from a list of high-confidence cancer drivers (Tamborero et al., 2013), and from a list of significantly mutated genes in cancer (Kandoth et al., 2013) and compared them with our list of *H. pylori*-susceptible regions in expressed genes. Performing hypergeometric distribution testing, we found 20 of these cancer-related genes to be enriched in our data (Table 1; $p = 0.01$).

Genomic Regions Accumulating DNA Damage Are Characteristic to *H. pylori* Infection but Are Not Cell-Type Specific

To analyze whether the damage pattern was unique to AGS cells, we examined *H. pylori*-susceptible regions in MKN74 cells. We chose a region with a strong increase in *H. pylori*-induced damage at the q-arm of chromosome 8, where the damage spread up to 5 Mb into subtelomeric regions as early as 6-hr p.i. (Figure 4A). We validated different regions and observed spreading of the signal after infection throughout all tested regions, while commonly used control regions at the myoglobin and *GAPDH* loci did not show increased signals (Lin et al., 2009; Smeenk et al., 2008) (Figures 4B, S3A, and S3B). Telomere-proximal regions on different chromosomes showed slight variations, but a clear increase in γH2AX accumulation was seen at 18-hr p.i. at all tested sites, while IR-induced γH2AX did not accumulate to significantly higher levels than the control region at the myoglobin locus (Figure 4C). We also included two putative IR-specific regions (Figure S3C), but did not see damage enrichment at these sites after infection, while IR introduced some γH2AX-accumulation at all of them, yet to an extent similar to the other control regions.

To exclude that the effects were due to the transformed nature of the cell lines, we extended the study to primary gastric cultures. Regions identified in AGS cells were also positive in non-transformed human cells and clearly enriched compared with the signal caused by IR (Figure 4D). We then analyzed the effects of *H. pylori* on known cancer-related genes localized to the damaged regions. Following our validation, we identified clear damage enrichment after infection in all but one (*ZMYND8*) of the regions tested (Figure 4E). Furthermore, we examined whether different genotoxic agents could induce γH2AX accumulation at the *H. pylori*-susceptible sites despite the differences in DDR pathway activation. Of particular interest were the effects of H_2O_2, since reactive oxygen species (ROS) are part of the innate cellular immune response triggered upon infection and could be responsible for the observed pattern of genomic damage. Adding N-acetyl-cystein (Nac) to quench H_2O_2 only led to a

moderate reduction of damage (Figure S3D). Treating MKN74 cells with the chemotoxin etoposide or H_2O_2 to induce an overall comparable amount of DSBs (Figures 1A and 4F) only induced very slight increases in DNA damage at *H. pylori*-susceptible sites compared with control regions, which was clearly exceeded by the *H. pylori*-induced damage at all susceptible regions (Figure 4F, right). Therefore, unlike other agents, *H. pylori* induces damage preferentially at specific susceptible regions regardless of the particular cell type tested.

DISCUSSION

We observed a unique pattern of DNA damage in host cells infected with *H. pylori*. By comparing the consequences for the host cell genome to those induced by other mutagenic agents, we find clear differences in the location and characteristics of DNA damage accumulation. Only infection-induced damage shows a clear correlation with transcribed regions, enrichment at the ends of chromosomal arms and correlation with chromosomal aberrations in gastric cancer genomes and known cancer genes. IR-induced damage, although comparable in size, was distributed mostly randomly. Since the location of the *H. pylori*-induced damage was similar in different cells, including non-transformed primary gastric epithelial cells, it is likely that a common mechanism underlies these events, e.g., the repression of certain stress response or repair pathways, suggesting that its occurrence is not restricted to a particular genetic state. In support of this, we observed a unique response of host cells to DNA damage by *H. pylori* with reduced activities of most proteins tested and multiple repair factors showing reduced expression.

Several effects of *H. pylori* on genomic integrity have been described. Downregulation of proteins involved in mismatch repair (Kim et al., 2002) together with aberrant activity of mutation causing deaminating enzymes (Matsumoto et al., 2007) might cause increased point mutation rates. Additionally, DSBs trigger the recruitment of other DDR proteins (Chaturvedi et al., 2011; Toller et al., 2011). We extend these observations by showing that, while some DDR-proteins are recruited to damaged sites, components of several other DNA repair pathways are specifically inhibited by the infection, including the previously reported mismatch repair factors. We also observed the inhibition of multiple factors involved in the response to replicative stress, including ATR and its interacting protein ATRIP (Zeman and Cimprich, 2014) at the level of protein modification and transcription. This might explain the damage accumulation at telomeres, which has previously been linked to replicative stress (Seo et al., 2012). Moreover, activation of MRE11 and NBS1, crucial for some DDR pathways, is inhibited, suggesting an insufficient response to the damage. Together with the recruitment of 53BP1 and the induction of G1 arrest (Daley and Sung, 2014; Ding et al., 2008; Kim et al., 2010), this suggests a shift in repair away from homologous recombination, which is usually driven by the MRN complex, toward non-homologous end joining (NHEJ), possibly leading to a more error-prone repair (Bunting et al., 2010; Shibata et al., 2014).

In our experimental setting, the genomic damage induced by *H. pylori* was partly cagPAI dependent, probably because it leads to reduced abundance of NBS1 and possibly also inhibition of other DDR pathways, e.g., by phosphorylation of MRE11. CagPAI is required for the induction of CIN (Umeda et al., 2009) and increases the cancer risk conferred by *H. pylori* infection (Blaser et al., 1995; Parsonnet et al., 1997). It causes upregulation of spermine oxidase (SMO), resulting in increased production of H_2O_2 and probably additional DNA damage (Chaturvedi et al., 2011), although one report found it to be dispensable for the induction of DSBs (Toller et al., 2011). These differences might be explained by differential experimental systems, such as the different strain or much higher MOI used in their study, which may mask cagPAI-dependent effects. While cagPAI-negative strains caused some DNA damage in our cell lines, this damage was not observed in our setting with primary cells.

We found a strong correlation of damaged regions with annotated genes and active transcription, in line with a reported correlation of gene expression with genomic rearrangements in several cancers (Drier et al., 2013; Stephens et al., 2009). The consequences of such gene damage upon infection might be more severe for those that have already been implicated in cancer (Futreal et al., 2004; Kandoth et al., 2013; Tamborero et al., 2013). We further found that chromosomal aberrations in gastric cancers show a similar distribution across the chromosomal arms and that recurring focal amplifications correlate significantly with the regions identified in our study (TCGA Research Network, 2014a; Wang et al., 2014). This strongly indicates that some of the structural genomic events in adenocarcinomas of the stomach could be directly caused by the infection. Interestingly, among the other datasets we analyzed, only genomic aberrations from prostate cancer resemble the pattern we observed with *H. pylori* (Baca et al., 2013; Berger et al., 2012; TCGA Research Network, 2014b). The influence of other bacterial infections on human cancers, like *P. acnes* in prostate cancer, is currently under debate, and our findings are certainly in congruence with the induction of specific bacteria-induced genomic patterns in host cell genomes. Additionally, the massive DNA damage close to the chromosomal ends could trigger loss of telomeres and CIN (Lo et al., 2002) and lead to genomic translocations and amplifications via breakage-fusion-bridge cycles (Bunting and Nussenzweig, 2013; Tanaka and Yao, 2009). It has been suggested that such events occur in gastric tumors (Hillmer et al., 2011) and the resulting aberrations cover larger genomic regions and thus may have more severe consequences than intra-chromosomal breaks (Dulak et al., 2012; Zack et al., 2013). We found that this telomere-proximal DNA damage accumulation was most prominent toward the end of the q-arm of chromosome 8, a region significantly amplified in adenocarcinomas of the stomach and esophagus and in relative proximity to the *MYC* oncogene frequently amplified in such cancers (Dulak et al., 2012).

However, several questions await further elucidation. It is likely that genomic aberrations caused by improper repair in vivo are maintained only rarely. It is also not known how many cells survive the infection and whether a particular target cell type is prone to give rise to cancer initiating cells. While evidence suggests that it takes several decades of infection before neoplastic changes emerge, cancer-related mutations may

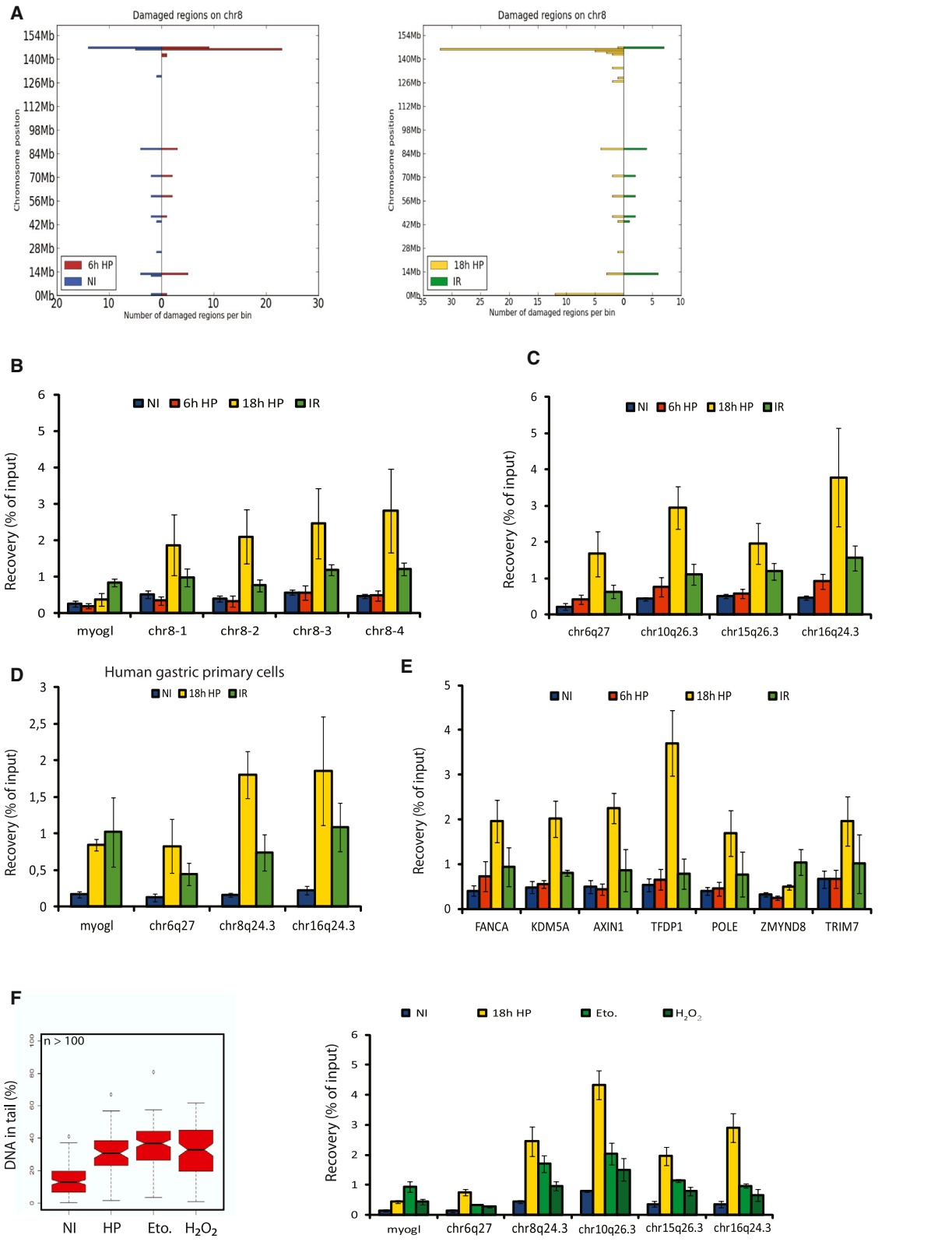

(legend on next page)

occur frequently. Whether such mutations escape the highly effective control mechanisms of our bodies, including cellular checkpoints and immune surveillance, is a matter of stochastics superimposed, e.g., by the age-dependent decline. Our work provides insight into the early genomic events upon infection and describes unique patterns of genomic damage and characterizes host genomic regions at higher risk of being damaged and therefore predisposed to genetic alterations.

EXPERIMENTAL PROCEDURES

Human Samples, Primary Cell Culture, and Bacterial Strains

Human gastric samples were provided by the Clinics for General, Visceral and Transplant Surgery and the Center of Bariatric and Metabolic Surgery, Charité University Hospital, Berlin and the University Clinic for Gastroenterology, Magdeburg. Usage of the samples for experimental purposes was approved by the Ethics Commission of the Charité, Berlin (EA1/058/11 and EA1/129/12) and the Ethics Commission of the Otto-Guericke University Magdeburg (80/11). Tissues were sourced from standard surgical procedures during sleeve resections or endoscopic biopsies. Culture and infection of primary material isolated from gastric glands were performed as described (Schlaermann et al., 2014). The following bacterial strains were used in this study: *H. pylori* strains P12 (strain collection number 243) and its derivatives P12ΔPAI (number P387), P12ΔVacA (number P216), and P12ΔCagA (number 378), as described by Koch et al. (2012).

RNA-seq and Analysis

Strand-specific paired-end RNA-seq libraries were sequenced on an Illumina HiSeq2500, mapped with Tophat2 and analyzed with Cufflinks (Trapnell et al., 2012).

ChIP, ChIP-seq, and Data Analysis

ChIP with an anti-γH2AX-ab (05-636; Millipore) was done according to Smeenk et al. (2008); primers for ChIP-qPCR are listed in Table S2. Libraries for ChIP-seq were constructed with the Nugen-Kit (Nugen Part number 0330, 0331) from 20 ng of precipitated DNA and sequenced on an Illumina HiSeq2500. After quality control and mapping, enriched region calling was performed using HOMER (Heinz et al., 2010), and comparative genomic analysis was done with the Galaxy Hyperbrowser.

Full details of experimental procedures are provided in the Supplemental Information.

ACCESSION NUMBERS

The accession number for the ChIP-sequencing data reported in this paper is GEO: GSE55699.

SUPPLEMENTAL INFORMATION

Supplemental Information includes Supplemental Experimental Procedures, three figures, and two tables and can be found with this article online at http://dx.doi.org/10.1016/j.celrep.2015.05.030.

AUTHOR CONTRIBUTIONS

M.K. and T.F.M. designed the experiments. M.K., F.G., and P.S. performed the experiments. F.G. and M.K. performed the gene expression analysis. M.K. and F.G.-A. assembled the analytical pipeline. F.G.-A. and M.K. analyzed the data. M.K. and F.G.-A. prepared the manuscript, and T.F.M. supervised the project.

ACKNOWLEDGMENTS

The authors thank K. Okonechnikov and M. Meyer for Bioinformatic support, D. Khalil and A. Greiser for excellent technical assistance, R. Zietlow for editing the manuscript, D. Schad for assistance with preparation of the graphical abstract, and R. Reinhardt and the Max Planck Genome Centre Cologne (http://mpgc.mpipz.mpg.de/home/) for performing all deep sequencing presented in this study. This work was supported by the Max Planck Innovationsfond for next generation sequencing.

Received: November 14, 2014
Revised: March 10, 2015
Accepted: May 16, 2015
Published: June 11, 2015

REFERENCES

Baca, S.C., Prandi, D., Lawrence, M.S., Mosquera, J.M., Romanel, A., Drier, Y., Park, K., Kitabayashi, N., MacDonald, T.Y., Ghandi, M., et al. (2013). Punctuated evolution of prostate cancer genomes. Cell *153*, 666–677.

Backert, S., Ziska, E., Brinkmann, V., Zimny-Arndt, U., Fauconnier, A., Jungblut, P.R., Naumann, M., and Meyer, T.F. (2000). Translocation of the Helicobacter pylori CagA protein in gastric epithelial cells by a type IV secretion apparatus. Cell. Microbiol. *2*, 155–164.

Barlow, J.H., Faryabi, R.B., Callén, E., Wong, N., Malhowski, A., Chen, H.T., Gutierrez-Cruz, G., Sun, H.W., McKinnon, P., Wright, G., et al. (2013). Identification of early replicating fragile sites that contribute to genome instability. Cell *152*, 620–632.

Bauer, B., and Meyer, T.F. (2011). The human gastric pathogen *Helicobacter pylori* and its association with gastric cancer and ulcer disease. Ulcers *2011*, ID 340157.

Berger, M.F., Hodis, E., Heffernan, T.P., Deribe, Y.L., Lawrence, M.S., Protopopov, A., Ivanova, E., Watson, I.R., Nickerson, E., Ghosh, P., et al. (2012).

Figure 4. *H. pylori*-Susceptible Genomic Regions Are Shared between Different Cell Types and Are Specific to the Infection

(A) γH2AX-signal from ChIP-seq in AGS cells displayed over equal bins of chromosome 8, showing damage accumulation as identified by HOMER. Visualized are the accumulated signals from both replicates for non-infected (blue), 6-hr infected (red), 18-hr infected (yellow), and irradiated cells (green), with a strong increase in signal for both infection time points.

(B) Validation of regions on chromosome 8 identified by γH2AX-ChIP-seq. MKN74 cells were treated as in (A) before ChIP and qPCR analysis. Signal is shown as recovery (percentage of input), resulting in an increase of signal from the tested loci on chr8. Myoglobin served as a negative control; error bars indicate SD from three independent experiments.

(C) Additional validation of regions preferentially damaged during infection. MKN74 cells were treated as in (A), and signals at *H. pylori*-susceptible regions were validated by ChIP-qPCR, showing the validation of identified regions at 18-hr p.i.; error bars indicate SD from three independent experiments.

(D) ChIP-qPCR in primary human gastric epithelial cells infected with P12 for 18 hr or subjected to 10 Gy IR. Shown are three previously identified loci which display enrichment of DNA damage signal after infection. Error bars represent SD derived from two independent experiments.

(E) Loci harboring known cancer genes were tested for bacterial-induced DNA damage. MKN74 cells were treated as in (A) for validation by ChIP-qPCR. Error bars indicate SD from three independent experiments.

(F) Damage induced by *H. pylori* is compared to other genotoxic agents. MKN74 cells were infected for 18 hr with P12 (MOI 50) or treated as indicated, before analyzing extent of DSBs by comet assay (left). Region specificity was tested by ChIP-qPCR (right). Only *H. pylori* caused a clear increase in damage-signal at the tested loci. Myoglobin served as negative control. Error bars indicate SD derived from three independent experiments.

See also Figure S3 and Table S2.

Melanoma genome sequencing reveals frequent PREX2 mutations. Nature *485*, 502–506.

Blaser, M.J., Perez-Perez, G.I., Kleanthous, H., Cover, T.L., Peek, R.M., Chyou, P.H., Stemmermann, G.N., and Nomura, A. (1995). Infection with Helicobacter pylori strains possessing cagA is associated with an increased risk of developing adenocarcinoma of the stomach. Cancer Res. *55*, 2111–2115.

Bunting, S.F., and Nussenzweig, A. (2013). End-joining, translocations and cancer. Nat. Rev. Cancer *13*, 443–454.

Bunting, S.F., Callén, E., Wong, N., Chen, H.T., Polato, F., Gunn, A., Bothmer, A., Feldhahn, N., Fernandez-Capetillo, O., Cao, L., et al. (2010). 53BP1 inhibits homologous recombination in Brca1-deficient cells by blocking resection of DNA breaks. Cell *141*, 243–254.

TCGA Research Network (2014a). Comprehensive molecular characterization of gastric adenocarcinoma. Nature *513*, 202–209.

TCGA Research Network (2014b). Comprehensive molecular profiling of lung adenocarcinoma. Nature *511*, 543–550.

Chaturvedi, R., Asim, M., Romero-Gallo, J., Barry, D.P., Hoge, S., de Sablet, T., Delgado, A.G., Wroblewski, L.E., Piazuelo, M.B., Yan, F., et al. (2011). Spermine oxidase mediates the gastric cancer risk associated with Helicobacter pylori CagA. Gastroenterology *141*, 1696–1708.e1-2.

Correa, P., and Piazuelo, M.B. (2012). The gastric precancerous cascade. J. Dig. Dis. *13*, 2–9.

Crosetto, N., Mitra, A., Silva, M.J., Bienko, M., Dojer, N., Wang, Q., Karaca, E., Chiarle, R., Skrzypczak, M., Ginalski, K., et al. (2013). Nucleotide-resolution DNA double-strand break mapping by next-generation sequencing. Nat. Methods *10*, 361–365.

Daley, J.M., and Sung, P. (2014). 53BP1, BRCA1, and the choice between recombination and end joining at DNA double-strand breaks. Mol. Cell. Biol. *34*, 1380–1388.

Ding, S.Z., Smith, M.F., Jr., and Goldberg, J.B. (2008). Helicobacter pylori and mitogen-activated protein kinases regulate the cell cycle, proliferation and apoptosis in gastric epithelial cells. J. Gastroenterol. Hepatol. *23*, e67–e78.

Drier, Y., Lawrence, M.S., Carter, S.L., Stewart, C., Gabriel, S.B., Lander, E.S., Meyerson, M., Beroukhim, R., and Getz, G. (2013). Somatic rearrangements across cancer reveal classes of samples with distinct patterns of DNA breakage and rearrangement-induced hypermutability. Genome Res. *23*, 228–235.

Dulak, A.M., Schumacher, S.E., van Lieshout, J., Imamura, Y., Fox, C., Shim, B., Ramos, A.H., Saksena, G., Baca, S.C., Baselga, J., et al. (2012). Gastrointestinal adenocarcinomas of the esophagus, stomach, and colon exhibit distinct patterns of genome instability and oncogenesis. Cancer Res. *72*, 4383–4393.

Fox, J.G., and Wang, T.C. (2007). Inflammation, atrophy, and gastric cancer. J. Clin. Invest. *117*, 60–69.

Futreal, P.A., Coin, L., Marshall, M., Down, T., Hubbard, T., Wooster, R., Rahman, N., and Stratton, M.R. (2004). A census of human cancer genes. Nat. Rev. Cancer *4*, 177–183.

Glover, T.W. (2006). Common fragile sites. Cancer Lett. *232*, 4–12.

Harrigan, J.A., Belotserkovskaya, R., Coates, J., Dimitrova, D.S., Polo, S.E., Bradshaw, C.R., Fraser, P., and Jackson, S.P. (2011). Replication stress induces 53BP1-containing OPT domains in G1 cells. J. Cell Biol. *193*, 97–108.

Hatakeyama, M. (2014). Helicobacter pylori CagA and gastric cancer: a paradigm for hit-and-run carcinogenesis. Cell Host Microbe *15*, 306–316.

Heinz, S., Benner, C., Spann, N., Bertolino, E., Lin, Y.C., Laslo, P., Cheng, J.X., Murre, C., Singh, H., and Glass, C.K. (2010). Simple combinations of lineage-determining transcription factors prime cis-regulatory elements required for macrophage and B cell identities. Mol. Cell *38*, 576–589.

Hillmer, A.M., Yao, F., Inaki, K., Lee, W.H., Ariyaratne, P.N., Teo, A.S., Woo, X.Y., Zhang, Z., Zhao, H., Ukil, L., et al. (2011). Comprehensive long-span paired-end-tag mapping reveals characteristic patterns of structural variations in epithelial cancer genomes. Genome Res. *21*, 665–675.

Jenks, P.J., Jeremy, A.H., Robinson, P.A., Walker, M.M., and Crabtree, J.E. (2003). Long-term infection with Helicobacter felis and inactivation of the tumour suppressor gene p53 cumulatively enhance the gastric mutation frequency in Big Blue transgenic mice. J. Pathol. *201*, 596–602.

Kandoth, C., McLellan, M.D., Vandin, F., Ye, K., Niu, B., Lu, C., Xie, M., Zhang, Q., McMichael, J.F., Wyczalkowski, M.A., et al. (2013). Mutational landscape and significance across 12 major cancer types. Nature *502*, 333–339.

Kim, J.J., Tao, H., Carloni, E., Leung, W.K., Graham, D.Y., and Sepulveda, A.R. (2002). Helicobacter pylori impairs DNA mismatch repair in gastric epithelial cells. Gastroenterology *123*, 542–553.

Kim, K.M., Lee, S.G., Kim, J.M., Kim, D.S., Song, J.Y., Kang, H.L., Lee, W.K., Cho, M.J., Rhee, K.H., Youn, H.S., and Baik, S.C. (2010). Helicobacter pylori gamma-glutamyltranspeptidase induces cell cycle arrest at the G1-S phase transition. J. Microbiol. *48*, 372–377.

Koch, M., Mollenkopf, H.J., Klemm, U., and Meyer, T.F. (2012). Induction of microRNA-155 is TLR- and type IV secretion system-dependent in macrophages and inhibits DNA-damage induced apoptosis. Proc. Natl. Acad. Sci. USA *109*, E1153–E1162.

Landt, S.G., Marinov, G.K., Kundaje, A., Kheradpour, P., Pauli, F., Batzoglou, S., Bernstein, B.E., Bickel, P., Brown, J.B., Cayting, P., et al. (2012). ChIP-seq guidelines and practices of the ENCODE and modENCODE consortia. Genome Res. *22*, 1813–1831.

Lange, S.S., Takata, K., and Wood, R.D. (2011). DNA polymerases and cancer. Nat. Rev. Cancer *11*, 96–110.

Lin, C., Yang, L., Tanasa, B., Hutt, K., Ju, B.G., Ohgi, K., Zhang, J., Rose, D.W., Fu, X.D., Glass, C.K., and Rosenfeld, M.G. (2009). Nuclear receptor-induced chromosomal proximity and DNA breaks underlie specific translocations in cancer. Cell *139*, 1069–1083.

Lo, A.W., Sprung, C.N., Fouladi, B., Pedram, M., Sabatier, L., Ricoul, M., Reynolds, G.E., and Murnane, J.P. (2002). Chromosome instability as a result of double-strand breaks near telomeres in mouse embryonic stem cells. Mol. Cell. Biol. *22*, 4836–4850.

Matsumoto, Y., Marusawa, H., Kinoshita, K., Endo, Y., Kou, T., Morisawa, T., Azuma, T., Okazaki, I.M., Honjo, T., and Chiba, T. (2007). Helicobacter pylori infection triggers aberrant expression of activation-induced cytidine deaminase in gastric epithelium. Nat. Med. *13*, 470–476.

Odenbreit, S., Püls, J., Sedlmaier, B., Gerland, E., Fischer, W., and Haas, R. (2000). Translocation of Helicobacter pylori CagA into gastric epithelial cells by type IV secretion. Science *287*, 1497–1500.

Parsonnet, J., Friedman, G.D., Orentreich, N., and Vogelman, H. (1997). Risk for gastric cancer in people with CagA positive or CagA negative Helicobacter pylori infection. Gut *40*, 297–301.

Peek, R.M., Jr., and Crabtree, J.E. (2006). Helicobacter infection and gastric neoplasia. J. Pathol. *208*, 233–248.

Pombo, A., Cuello, P., Schul, W., Yoon, J.B., Roeder, R.G., Cook, P.R., and Murphy, S. (1998). Regional and temporal specialization in the nucleus: a transcriptionally-active nuclear domain rich in PTF, Oct1 and PIKA antigens associates with specific chromosomes early in the cell cycle. EMBO J. *17*, 1768–1778.

Schlaermann, P., Toelle, B., Berger, H., Schmidt, S.C., Glanemann, M., Ordemann, J., Bartfeld, S., Mollenkopf, H.J., and Meyer, T.F. (2014). A novel human gastric primary cell culture system for modelling Helicobacter pylori infection in vitro. Gut., Published online December 24, 2014 http://dx.doi.org/10.1136/gutjnl-2014-307949.

Seo, J., Kim, S.C., Lee, H.S., Kim, J.K., Shon, H.J., Salleh, N.L., Desai, K.V., Lee, J.H., Kang, E.S., Kim, J.S., and Choi, J.K. (2012). Genome-wide profiles of H2AX and γ-H2AX differentiate endogenous and exogenous DNA damage hotspots in human cells. Nucleic Acids Res. *40*, 5965–5974.

Shibata, A., Moiani, D., Arvai, A.S., Perry, J., Harding, S.M., Genois, M.M., Maity, R., van Rossum-Fikkert, S., Kertokalio, A., Romoli, F., et al. (2014). DNA double-strand break repair pathway choice is directed by distinct MRE11 nuclease activities. Mol. Cell *53*, 7–18.

Smeenk, L., van Heeringen, S.J., Koeppel, M., van Driel, M.A., Bartels, S.J., Akkers, R.C., Denissov, S., Stunnenberg, H.G., and Lohrum, M. (2008). Characterization of genome-wide p53-binding sites upon stress response. Nucleic Acids Res. *36*, 3639–3654.

Stephens, P.J., McBride, D.J., Lin, M.L., Varela, I., Pleasance, E.D., Simpson, J.T., Stebbings, L.A., Leroy, C., Edkins, S., Mudie, L.J., et al. (2009). Complex landscapes of somatic rearrangement in human breast cancer genomes. Nature *462*, 1005–1010.

Tamborero, D., Gonzalez-Perez, A., Perez-Llamas, C., Deu-Pons, J., Kandoth, C., Reimand, J., Lawrence, M.S., Getz, G., Bader, G.D., Ding, L., and Lopez-Bigas, N. (2013). Comprehensive identification of mutational cancer driver genes across 12 tumor types. Sci. Rep. *3*, 2650.

Tanaka, H., and Yao, M.C. (2009). Palindromic gene amplification—an evolutionarily conserved role for DNA inverted repeats in the genome. Nat. Rev. Cancer *9*, 216–224.

Toller, I.M., Neelsen, K.J., Steger, M., Hartung, M.L., Hottiger, M.O., Stucki, M., Kalali, B., Gerhard, M., Sartori, A.A., Lopes, M., and Müller, A. (2011). Carcinogenic bacterial pathogen Helicobacter pylori triggers DNA double-strand breaks and a DNA damage response in its host cells. Proc. Natl. Acad. Sci. USA *108*, 14944–14949.

Touati, E., Michel, V., Thiberge, J.M., Wuscher, N., Huerre, M., and Labigne, A. (2003). Chronic Helicobacter pylori infections induce gastric mutations in mice. Gastroenterology *124*, 1408–1419.

Trapnell, C., Roberts, A., Goff, L., Pertea, G., Kim, D., Kelley, D.R., Pimentel, H., Salzberg, S.L., Rinn, J.L., and Pachter, L. (2012). Differential gene and transcript expression analysis of RNA-seq experiments with TopHat and Cufflinks. Nat. Protoc. *7*, 562–578.

Umeda, M., Murata-Kamiya, N., Saito, Y., Ohba, Y., Takahashi, M., and Hatakeyama, M. (2009). Helicobacter pylori CagA causes mitotic impairment and induces chromosomal instability. J. Biol. Chem. *284*, 22166–22172.

Wang, K., Kan, J., Yuen, S.T., Shi, S.T., Chu, K.M., Law, S., Chan, T.L., Kan, Z., Chan, A.S., Tsui, W.Y., et al. (2011). Exome sequencing identifies frequent mutation of ARID1A in molecular subtypes of gastric cancer. Nat. Genet. *43*, 1219–1223.

Wang, K., Yuen, S.T., Xu, J., Lee, S.P., Yan, H.H., Shi, S.T., Siu, H.C., Deng, S., Chu, K.M., Law, S., et al. (2014). Whole-genome sequencing and comprehensive molecular profiling identify new driver mutations in gastric cancer. Nat. Genet. *46*, 573–582.

Zack, T.I., Schumacher, S.E., Carter, S.L., Cherniack, A.D., Saksena, G., Tabak, B., Lawrence, M.S., Zhang, C.Z., Wala, J., Mermel, C.H., et al. (2013). Pan-cancer patterns of somatic copy number alteration. Nat. Genet. *45*, 1134–1140.

Zang, Z.J., Cutcutache, I., Poon, S.L., Zhang, S.L., McPherson, J.R., Tao, J., Rajasegaran, V., Heng, H.L., Deng, N., Gan, A., et al. (2012). Exome sequencing of gastric adenocarcinoma identifies recurrent somatic mutations in cell adhesion and chromatin remodeling genes. Nat. Genet. *44*, 570–574.

Zeman, M.K., and Cimprich, K.A. (2014). Causes and consequences of replication stress. Nat. Cell Biol. *16*, 2–9.